Cite as: Matcovitch-Natan *et al.*,
Science 10.1126/science.aad8670 (2016).

Microglia development follows a stepwise program to regulate brain homeostasis

Orit Matcovitch-Natan,[1,2]* Deborah R. Winter,[1]* Amir Giladi,[1] Stephanie Vargas Aguilar,[3,4,5,6] Amit Spinrad,[1,2] Sandrine Sarrazin,[3,4,5] Hila Ben-Yehuda,[2] Eyal David,[1] Fabiola Zelada González,[3,4,5] Pierre Perrin,[3,4,5] Hadas Keren-Shaul,[1] Meital Gury,[1] David Lara-Astaiso,[1] Christoph A. Thaiss,[1] Merav Cohen,[2] Keren Bahar Halpern,[7] Kuti Baruch,[2] Aleksandra Deczkowska,[2] Erika Lorenzo-Vivas,[1] Shalev Itzkovitz,[7] Eran Elinav,[1] Michael H. Sieweke,[3,4,5,6]†‡ Michal Schwartz,[2]†‡ Ido Amit[1]†‡

[1]Department of Immunology, Weizmann Institute of Science, Rehovot, Israel. [2]Department of Neurobiology, Weizmann Institute of Science, Rehovot, Israel. [3]Centre d'Immunologie de Marseille-Luminy, Université Aix-Marseille, UM2, Campus de Luminy, Marseille, France. [4]Institut National de la Santé et de la Recherche Médicale (INSERM), U1104, Marseille, France. [5]Centre National de la Recherche Scientifique (CNRS), UMR7280, Marseille, France. [6]Max-Delbrück-Centrum für Molekulare Medizin in der Helmholtz-Gemeinschaft (MDC), Robert-Rössle-Straß 10, 13125 Berlin, Germany. [7]Department of Cell Biology, Weizmann Institute of Science, Rehovot, Israel.

*These authors contributed equally to this work.

†These authors contributed equally to this work.

‡Corresponding author. Email: sieweke@ciml.univ-mrs.fr (M.H.S.); Michal.Schwartz@weizmann.ac.il (M.S.); ido.amit@weizmann.ac.il (I.A.)

Microglia, the resident myeloid cells of the central nervous system, play important roles in life-long brain maintenance and in pathology. Despite their crucial role, their regulatory dynamics during brain development have not been fully elucidated. Genome-wide chromatin and expression profiling coupled with single-cell transcriptomic analysis throughout development reveal that microglia undergo three temporal developmental stages in synchrony with the brain: early, pre-, and adult microglia, which are under distinct regulatory circuits. Knockout of the adult microglia transcription factor MafB and environmental perturbations, such as those affecting the microbiome or prenatal immune activation, led to disruption of developmental genes and immune response pathways. Together, our work identifies a stepwise developmental program of microglia integrating immune response pathways that may be associated with several neurodevelopmental disorders.

Microglia are the resident myeloid cells of the central nervous system (CNS) that control the patterning and wiring of the brain in early development and contribute to homeostasis throughout life (*1–3*). In the embryo, starting at day 8.5 post-conception (E8.5), erythromyeloid progenitors (EMPs) develop in the yolk sac: these cells are CD45+ cKit+ and have the capacity to colonize the fetal liver and differentiate into erythrocytes and various myeloid cells, including tissue-resident macrophages (*4*). A subset of EMPs matures into CX3CR1+ cells in the yolk sac and become microglia progenitors (*5*, *6*). These progenitors migrate to the brain starting at days E9.5-10.5 and may continue until the formation of the blood-brain barrier at day E13.5-14.5 (*4*, *7*). The microglia population proliferates locally within the brain, and distributes spatially in the central nervous system (*8*, *9*). This original pool of cells is the only source of myeloid cells in the healthy brain (*10*, *11*). Other myeloid cells, such as bone marrow-derived monocytes, only infiltrate the brain under pathological circumstances (*6*, *12–14*).

Myeloid cells, particularly macrophages, are endowed with a higher plasticity than was previously appreciated. They engage in a bi-directional dialogue with their microenvironment, which both shapes their fate and is influenced by their activity (*15*, *16*). In the brain, exposure to TGFB1, which acts through the Smad and the Irf7 pathway, has been shown to shape the chromatin landscape and influence the response and phenotype of microglia (*17–20*). In combination with environmental signals, general lineage-specific factors, such as Pu.1 and Irf8, define the microglial regulatory network and distinguish it from other macrophages (*7*, *15*, *16*). The evolution of the microglia regulatory network may also be shaped by multiple tissue-specific signals, including protein aggregates, stress signals, nutrients, as well as the communities of commensal microorganisms colonizing the skin, respiratory, gastrointestinal, and urogenital tract – collectively termed the microbiota (*21*, *22*) The collection of physiological and pathological cues sensed by microglia – originating from within the brain or externally (*21*), may fluctuate spatially across the different brain regions and temporally with development of the brain. Thus, microglial programming must be complex enough to process dynamic environmental signals and execute the necessary temporal function to accommodate the brain's needs throughout development and adulthood.

It is still unknown how one cell type displays the necessary functional diversity to meet both the needs of the developing brain, as well as life-long maintenance. We hypothesized that microglia acquire specialized functions tailored to changes in the developing brain by a combination of gene regulation and response to environmental signals. Importantly, although microglia share many circuits with monocytes, they must maintain tight control of inflammatory and antiviral pathways in order to prevent neuronal damage, particularly under the various stress conditions that may influence the fetus during pregnancy (*23*). Presently, the expression programs and regulatory networks are only documented for early yolk sac progenitors and adult microglia (*2*, *7*, *15*, *16*, *19*, *24*). Microglia modulate synaptic transmission, formation, and elimination, and shape embryonic and postnatal brain circuits (*25–31*). However, many of these processes, such as synaptic pruning and neuronal maturation, peak in mice during the first week after birth – a period that has not yet been profiled in microglia (*27–31*)– and may be important to understanding the circuits and etiology of many neurodevelopmental diseases.

Perturbation of the microglia environment during development may alter the strict timing of developmental programs and lead to misplaced expression of gene pathways, such as inflammation, that disrupt neuronal development and lead to brain disorders at later stages in life (*30*). For example, prenatal exposure to viral infection has been correlated with an increased risk of schizophrenia and autism in mouse and human offspring (*32*, *33*). The precise effects of perturbations on development are highly dependent on the timing of infection, suggesting interference with specific processes (*34*, *35*).

Results

Temporal expression profiles during microglia development

To study the dynamics of the gene programs involved in microglia development, we performed RNA-seq to measure the global gene expression of myeloid progenitors from the yolk sac (*5*) and microglia from embryonic, post-natal, and adult brain (*36*) for a total of nine time points throughout microglia development (Fig. 1A and fig. S1). Biological replicates were highly correlated ($r>0.98$, Pearson's correlation) and few transcriptional changes were noted across adjacent time points (fig. S2A). Surprisingly, we found a large number of genes that were differentially expressed across developmental time points (Fig. 1B). Early microglia were associated with genes involved in cell cycle and differentiation, such as *Mcm5* and *Dab2* (*37*). In contrast, *Csf1, Cxcr2*, and other genes involved in neuronal development peaked in expression a few days before birth and decreased by adulthood. Canonical adult microglia genes, including *Cd14* and *Pmepa1*, were primarily expressed only in adult microglia.

Microglia development demonstrates discrete transcriptional phases

In order to identify global patterns of gene expression, we performed K-means clustering (k=7) that divided the data into 4 main categories on the basis of the developmental location and timing in which the genes were expressed (Fig. 1C; fig. S2, B and C; and table S1). We focused on 3059 of the most highly and differentially expressed genes throughout development (*38*). We defined these stages as early microglia (1289 genes, clusters E1-2, day E10.5 to E14), pre-microglia (589 genes, clusters P1-2, day E14 to P9), and adult microglia (808 genes, clusters A1-2, 4 weeks and onwards). Adult microglia exhibited only a small number of differentially expressed genes, (76 genes, table S2; (*38*)), across different CNS regions; cortex, hippocampus, and spinal cord. In addition, there was also a group of genes that are most highly expressed in the yolk sac (373 genes, cluster YS). Comparison of gene ontologies (GO) indicated that yolk-sac-specific genes were associated with defense response and multiple hematopoietic fates (e.g., *Lyz2* (*39*) and *Pf4* (*40*)), while shared clusters between yolk sac and early brain were enriched for genes associated with proliferation and cell cycle (fig. S2B). Notably, the yolk sac and early brain microglia showed high correlation at the transcriptional level over time, despite differences in microenvironment (fig. S2A). This observation suggests that either microglia newly arrived to the brain are not immediately adapting upon encountering the neural environment, or alternatively, that the first stage of microglia development commences in the yolk sac.

Interestingly, we observed that the pre-microglia stage reflects a distinct phenotype of characteristic genes. Because previous studies have focused on cells from more mature developmental stages, many of these genes have not been annotated with microglia function. However, we found here that a subset of the genes that were expressed at this stage was related to the GO categories of neural migration, neurogenesis, and cytokine secretion (fig. S2B). Based on the timing of the pre-microglia program, this phase probably represents when microglia adopt a role in synaptic pruning and neural maturation; later, when the brain matures, they enter a surveillance and homeostatic phase where they acquire functions associated with tissue maintenance and signaling (*41*) and express canonical microglia genes (fig. S2B). To confirm and strengthen the reproducibility of these microglia transcriptional stages, we applied dimension reduction analyses – nonnegative matrix factorization (NMF) (*38*, *42*) and principal component analysis (PCA) – to the RNA-seq data. NMF, which deconstructs the data into a given

number of metagenes, robustly uncovered 3 discrete expression programs coinciding with the three microglia stages (Fig. 1D and fig. S2, D to F). Similar results were obtained with PCA (fig. S1G). This partitioning suggests that the temporal expression profile of microglia development in the brain consists primarily of two major transition events: early microglia to pre microglia around embryonic day 13.5-14.5 and pre-microglia to adult microglia a few weeks after birth.

Microglia developmental phases are linked with changes in the chromatin landscape

The changing chromatin landscape across developmental time points can inform on the regulatory mechanisms underlying gene expression profiles. Accessible or 'open' chromatin regions contain regulatory elements that influence transcription in a cell-type-specific or condition-specific manner (*43*–*45*). We thus performed an assay for transposase accessible chromatin (ATAC (*46*)), as well as using a recently developed, highly sensitive method for chromatin immunoprecipitation followed by sequencing (iChIP, (*47*)), for each transcriptional stage: yolk sac, early microglia, pre-microglia, and adult microglia. Unlike the RNA-seq data, the chromatin landscape of early microglia was more closely related to that of pre-microglia than to yolk sac (fig. S3A), suggesting that chromatin changes precede changes in RNA (*47*). ATAC-seq identifies accessible regions within promoters (H3K4me3+ regions near the transcription start site of genes) and enhancers, distal regions associated with higher H3K4me1/2 (*48*, *49*), as well as other regulatory elements, such as CTCF binding sites (*46*). As seen previously (*16*), the accessibility of promoter regions is largely conserved over time (fig. S2B). Thus, we focused on candidate enhancers marked by distal ATAC-seq regions with high levels of H3K4me2, as assayed by iChIP (*47*). These enhancer regions could be divided into the 4 major categories, similar to the gene expression profiles (Fig. 2, A and B; fig. S3, C and D; and table S3). The first category was composed of enhancers marked only in the yolk sac (e.g., F13a1) and may reflect regions that are active in cells not migrating to the brain. Another category comprised enhancers accessible in both the early and pre-microglia, but not in adult microglia. The final categories consisted of enhancers that are most prominent in adult microglia and are distinguished by whether they are open (e.g., Sall1 and MafB) or closed (e.g., Irf8) earlier in development. Notably, no category was solely found in pre-microglia. This suggests that that the pre-microglia phase does not undergo unique chromatin remodeling, but rather exhibits differential usage of the epigenomic landscape established early in microglia development.

To confirm that the observed chromatin changes were related to transitions in microglia development, we assessed whether different enhancer dynamics were associated with the global expression patterns (Figs. 1C and 2B). We linked enhancers to genes by their proximity to the transcription start site (Fig. 2C and table S4, (*38*)). Genomic regions close to genes expressed in the early stage tended to be in the first two enhancer categories (Fig. 1C, clusters YS, E1-2). Similarly, the latter two categories were enriched for genes from the mature microglia transcriptional profile (Fig. 1C, clusters A1-2). The dynamics of the microglia enhancer repertoire confirm that the microglia gene expression across developmental stages does reflect shifts in the underlying chromatin landscape. However, it is important to note that with bulk data, such as from the RNA expression and chromatin profiling above, it is unclear whether the transcriptional signal represents the average profile of a heterogeneous mixture of cells from different phases or homogenous populations where each cell exhibits the relevant temporal profile.

Single cell transcriptome analysis reveals coordinated shifts between phases

In order to assess the heterogeneity at each temporal phase in microglia development, we performed massively parallel single cell RNA-seq (MARS-seq; (*50*)) on a representative time point from each phase. Then, we combined the data for cells from all phases and clustered them on the basis of their gene expression profiles (*51*). In order to correct for batch effects, each sample was normalized separately prior to clustering across time points (*38*). Clustering analysis of 2831 single cell profiles (696 from yolk sac, 734 from early, 705 from pre-, and 696 from adult) created a detailed map of 2071 differentially expressed genes across 16 transcriptionally homogeneous subpopulations (Fig. 3, A and B). The expression of key marker genes (Fig. 3B and fig. S4A) combined with global correlation analysis (fig. S4B) were used to examine the inter-cluster relationships of transcriptional subpopulations. We determined that each cluster originated almost entirely from a specific stage, confirming that the temporal dynamics of microglia development are the most dominant discriminative feature even at the single cell level (Fig. 3C). The exceptions were two subpopulations to which both the yolk sac and early brain time points contributed (fig. S4C, VII-VIII). It is possible that these subpopulations were composed of cells that were on the verge of or had just completed migration to the brain. Moreover, there was additional variation in the yolk-sac-specific subpopulation VI and, to a lesser degree, subpopulations II, III, and IV (Fig. 3, A and B, and fig. S4A), which displayed high expression of monocytic genes. When the single cell subpopulations were compared with the bulk RNA-seq time points (Fig. 1), we found that several of the yolk sac subpopulations (IV-VIII) were best matched to early microglia expression (fig. S4D). This suggests that the yolk sac population is heterogeneous

and may include both cells with other hematopoietic fates as well as cells with varying levels of commitment toward the microglia fate. Once in the brain, their further development occurs in a discrete stepwise fashion that is temporally regulated by environmental cues.

In general, the temporal gene markers we identified from the bulk RNA-seq analysis exhibited equivalent expression in the single cell data (Fig. 3B and fig. S4A). To confirm the stage-specific expression of marker genes (Fig. 3, D to F, upper left panel) in the intact brain, we imaged individual mRNA molecules using single-molecule fluorescent in situ hybridization (smFISH) in frozen brain sections from early, pre and adult stages (Fig. 3, D to F, and fig. S5A) (*52–54*). We found that Mcm5, Csf1, and MafB were each enriched in Cx3cr1+ microglia cells from the early, pre and adult brain, respectively. Using immunohistochemistry further confirmed that Dab2, a gene that had not been previously associated with microglia, is specifically expressed in early microglia (E12.5), but not at later time points (fig. S5, B and C). Further, Csf1R and Selplg show adult microglia expression in the Allen Brain Atlas (*55*) (fig. S5D). Taken together, these results indicate that coordinated transcriptional events control the transitions through microglia development and are likely due to changes in the microenvironment of the CNS.

Distinct transcription factors regulate microglia developmental phases

Transcription factors play important roles in regulating the chromatin state and gene expression of a cell (*56*, *57*). To investigate regulatory factors defining the temporal stages of microglia development, we focused on the expression of genes known to have a DNA binding or chromatin remodeling function and found candidate regulators for each stage (Fig. 4, A and B; fig. S6A; and table S5). In particular, cell cycle factors and chromatin remodelers were highly expressed in the early microglia stage. Canonical microglia transcription factors, such as Egr1 and Sall1, begin to be expressed in the pre-microglia stage and are further induced in adulthood. In contrast, we observe several regulators, including Jun, Fos, Mef2a, and MafB, that are specific to the adult stage and are therefore likely to be involved in establishing microglia homeostatic functions or in terminating developmental functions of pre-microglia (Fig. 4B and fig. S6A).

Motif analysis of the promoters associated with genes from the expression clusters (Fig. 1C) highlighted the differential occurrence of motifs for multiple transcription factors across microglia development (Fig. 4C, fig. S6B, and table S6), which coincided with the clusters exhibiting the highest expression of the genes encoding these factors. For example, the Mef2a motif was found to be enriched only in the regulatory regions of adult microglia genes. Previous work focusing on the mechanisms of tissue-resident macrophage specification also suggested the MEF2 family is important in microglia identity and may play a role in shaping the epigenomic landscape (*16*). Thus, changes in microglia function throughout development are likely linked to synchronized changes in the underlying regulatory networks.

MafB regulates adult microglia homeostasis

We further focused on the functional role of MafB, as one of the principal transcription factors to be highly elevated upon the shift from pre- to adult microglia (Figs. 1B, 3B, and 3F). Using immunohistochemistry, we confirmed that MafB is induced in the transition from pre- to adult microglia (Fig. 5A and fig. S7, A and B). MafB, was previously shown to be critical for terminal differentiation of monocytes and tissue-resident macrophages and to restrict their self-renewal capacity (*58–60*), In addition, the MAF motif was found to be enriched in macrophage-specific enhancers regions, suggesting it has the capacity to alter the chromatin landscape in a lineage-specific manner (*16*). However, the role of MafB in microglia development and homeostasis is not yet established.

To address the functional role of MafB in microglia development, we generated $MafB^{flox/flox}Csf1R^{Cre/+}$ transgenic mice that exhibit loss of MafB expression in the macrophage lineage (Fig. 5B and fig. S7, C to E), including microglia, but not in other cells in the CNS. We collected microglia from newborn (pre-microglia) and adult mice and compared their transcriptional profile to control mice ($MafB^{flox/flox}Csf1R^{+/+}$) of the same age. Successful knockout was confirmed by analyzing MafB expression levels (Fig. 5C). Consistent with the strong up-regulation of MafB in adult microglia, we observe a greater number of expression changes at the adult stage as opposed to the pre-microglia (Fig. 5, C to E; fig. S7F; and tables S7 and S10). Moreover, all categories of genes regulated by MafB were significantly enriched for genes expressed in late adult stage of microglia development, such as *Ctsh* and *Pmepa1* (cluster A2; $P<0.05$, hypergeometric distribution; Fig. 5, C and D, and fig. S7, G and H). Remarkably, genes that are up-regulated in both pre- and adult microglia included genes in the interferon-stat pathway, such as *Oas2, Mx1, Ifit3, Cxcl10* and *Il1b* (Fig. 5, C and D) and were associated with immune and viral Gene Ontology terms (fig. S7I). Together, these results reveal a role of MafB in suppressing antiviral response pathways and confirm its functional importance in regulating adult microglia homeostasis.

Germ-free mice contain microglia with an underdeveloped adult phenotype

To further substantiate the importance of microglia stepwise development program, we assessed how environmental

perturbations in specific stages might differentially affect microglia development and the associated genes. To this end, we chose the models of germ free (GF) conditions and maternal immune activation (MIA). Studies have shown that changes in the microbiome affect the immune system as well as the brain (*61*, *62*) and mice with dysbiosis have defects in their microglia population (*21*). To test whether the microbiome contributes to the environmental signals controlling microglia development, we sorted microglia from germ-free (GF) mice at the pre- (newborn) and adult stages and compared them to control mice of the same age housed in a conventional pathogen-free environment. We observed a greater number of genes that are down-regulated to a higher degree in adult microglia compared with newborn (322 vs. 240; Fig. 6, A and B; fig. S8, A to C; and tables S8 and S10), which may be explained by the change in microbiome composition at weaning (*63*, *64*). In line with previous reports (*21*), microglia from GF mice exhibited decreased expression of genes associated with inflammation and defense response (Fig. 6, B and C, and fig. S8, B and C). Importantly, genes associated with adult microglia (Fig. 6, A and B, and fig. S8C) were also perturbed in adult GF mice: of the down-regulated developmental genes, a significant fraction were part of our late adult microglia signature (cluster A2, 20 genes; $P=1.1*10^{-2}$, hypergeometric distribution). These results link the microbiome to the transition of microglia from the pre- to adult phenotype and suggest that microglia development is sensitive to perturbations influencing immune signals.

Microglia development is perturbed by immune activation during pregnancy

MIA by viral infection has been shown to cause neurodevelopmental defects in adult offspring, as well as behavioral deficits (*32*). Functional abnormalities in the brains of the progeny range from autism to schizophrenia, depending on the timing and conditions of the maternal infection (*35*). Transient exposure of pregnant mice to polyriboinosinic-polyribocytidilic acid (poly I:C) serves as an animal model that reproduces the human disease. Viral infection or poly I:C injection at different stages of the pregnancy leads to distinct neurodevelopmental disease in adulthood, which implicates the specific brain developmental process being executed at the time of intervention (*33–35*, *65*). In order to examine the effect of MIA on microglia development, we injected pregnant mice with poly I:C at day 14.5 post-conception (initiation of pre-microglia stage) and collected independent samples of microglia from the newborn and adult offspring of at least two mothers for RNA-seq analysis (fig. S8D and table S9).

In pre-microglia, 174 and 68 developmental genes exhibited at least 2-fold increased and decreased expression, respectively, in poly I:C offspring compared to PBS-injected controls (Fig. 6, D and E; fig. S8, E and F; and table S10) (*38*). Within this set, there was significant overlap between genes with increased expression in newborn offspring of mothers injected with poly I:C, and those from clusters expressed primarily in adult microglia (Fig. 1C, clusters A1-2), while depleted genes overlapped with clusters associated with early microglia (Fig. 1C, clusters E1-2). Similar results were seen in the comparable experiment with poly I:C injection at E12.5 (fig. S8G). Interestingly, we observed far fewer examples of differential expression in developmental genes at adult stage compared to the pre-microglia stage (fig. S8, E and F), suggesting the overall expression program of poly I:C mice was realigned with the normal phenotype at adulthood. This may explain why previous studies of adult microglia in MIA did not uncover microglia perturbations (*66*), and emphasizes that a transient perturbation in microglia development might have far reaching implications on the brain in adulthood. Overall, microglia from mice subjected to MIA and analyzed at the pre-microglia stage were transcriptionally shifted toward a more advanced developmental stage. We propose that such disruptions in the precise timing of microglia development may perturb their physiological functions in the developing brain and may explain neurodevelopmental diseases in later stages of development, long after microglia phenotype was restored.

Discussion

Tissue-resident cells of the immune system must exhibit plasticity in the face of a multitude of signals, while still maintaining tight regulation of tissue homeostatic functions. Microglia, as resident myeloid cells in an immune-privileged tissue, provide an ideal model for studying the crosstalk of immune cells with the surrounding environment during development. Once the blood-brain barrier is formed early in development, entry of other immune cells from the periphery is negligible, so the developmental effects on microglia can be solely attributed to the processes they undergo within the brain (*9*, *24*). Microglia are not only pivotal during CNS development, but are also responsible for brain homeostasis throughout life without allowing for deviation, such as aggressive inflammation. Here, we identified three distinct phases of regulatory networks in microglia and demonstrate how perturbation of this tight regulation leads to distinct functional effect.

On the basis of the present findings, we propose that the expression program of each phase has evolved to support the parallel development of the brain, while keeping in check local innate immune functions that may cause collateral damage. We might expect to see similar transitions in the resident myeloid cells of other tissues: for example, Kupffer cells, the resident macrophages of the liver (*24*, *67*).

Moreover, resident cells also receive changing signals from their environment as the tissue ages (e.g., increased apoptotic cells); these signals must also be controlled to avoid threatening responses. Our research highlights the importance of resident myeloid cell adaptation to the changing microenvironment throughout development and the potential for pathologies associated with perturbation of the regulatory circuitry through environmental signals, such as the microbiome or maternal immune activation.

Each stage in microglia development was found to be associated with different signals and functions: thus, the transitions between stages may represent a source of fragility of the system. Perturbations that target these transitions are likely to disrupt different processes depending on the timing, and may have impact on the homeostasis of the adult brain, as indicated by the dysregulation of the developmental expression patterns of immune response genes. For example, previous research has suggested that the immune system is adapted to natural changes in the microbiota composition due to weaning, which occurs in the first weeks after birth around the pre- to adult microglia shift (*61*, *63*, *64*, *68*). Our results suggest that in mice lacking these microbiome signals, microglia maturity is disrupted with down-regulation of genes associated with inflammation. These signals may reach the brain either directly through certain metabolites (*21*), or more likely, indirectly through the effect of systemic immunity on the barriers of the blood-brain interface (*69–71*). On the other hand, a transient maternal immune activation at 14.5 embryonic stage has the greatest effect on the pre-microglia stage and is accompanied by an up-regulation of inflammatory genes. Nevertheless, the resulting behavioral disorders are observed in the offspring at adulthood and may reflect the impact of the stage-specific microglia response on neurogenesis and synaptic pruning. Such perturbations likely act through distinct regulatory factors in each developmental phase.

MafB controls cell cycle arrest during terminal macrophage differentiation, whereas its absence is required for macrophage proliferation (*58–60*). Here, we identified the critical influence of MafB on the ability of microglia to express the adult gene program and its role in inflammatory regulation. Thus, MafB may represent an important "off" state factor for regulating the response of microglia under various stress conditions (*1*). In its absence, dozens of developmental genes are dysregulated and microglia adopt a dramatic antiviral response state. Interestingly, the role attributed here to MafB in microglia homeostasis was only possible to reveal in the context of distinct stages of microglia development. The relationship between MafB and the immune response has yet to be fully described, but previous work suggests that MafB may have an antagonistic relationship with the interferon pathway (*72*). This suggests that microglia-specific MafB-knockout mice may have increased penetrance of neurodevelopmental disease and a premature aging phenotype (*69*). Further work on MafB and identification of other signals and factors that contribute to microglia transitions and homeostasis will allow us to better understand the crosstalk between microglia and the CNS in both normal development and pathology.

In light of our results, as well as those emerging with respect to inhibitory factors such as programmed cell death protein 1 (PD-1), it is becoming clear that the immune system has developed at least as many inhibitory pathways for immune modulation as there are activating pathways (*73*). Further, these immune inhibitory pathways have likely evolved in a tissue-specific manner to curb immune activation and collateral damage in sensitive tissues such as the brain. These modulation pathways can be intrinsic (e.g., MafB) or extrinsic (PD-1) to the cell. A more thorough understanding of the crosstalk between microglia and other cells within the CNS, as well as the signals and pathways involved during development and aging, is essential to developing new approaches for intervention and improved diagnostics.

Materials and Methods

Animals

CX3CR1$^{GFP/+}$ (*74*) and wild-type C57/Bl6 mice were taken throughout development as indicated in the text with 2 replicates at each time point (with the exception of Brain E14, which combines samples from E13.5 and E14.5). Timed pregnancy was performed to obtain the embryos at defined time points after conception. Pregnant females with vaginal plugs were determined as 0.5 dpc. Adult mice were taken at 8 weeks. Animals were supplied by the Animal Breeding Center of the Weizmann Institute of Science. All animals were handled according to the regulations formulated by the Institutional Animal Care and Use Committee (IACUC).

Isolation of hematopoietic cells from yolk sac

Yolk sacs were dissected from staged embryos. Single cell suspensions were achieved using software-controlled sealed homogenization system (Dispomix; http://www.biocellisolation.com) in PBS. Cell suspensions were first blocked with Fc-block CD16/32 (BD Biosciences, San Jose, CA), and then stained for CD45^{+} (1: 150, 30-F11, biolegend Inc. San Diego, CA), CD11b^{+} (1:150, M1/70, biolegend Inc. San Diego, CA), and gated for CX3CR1-GFP positive. Cell populations were sorted with a SORP Aria.

Microglia harvesting

Naïve C57BL/6J female mice were bred overnight with CX3CR1$^{GFP/GFP}$ males (*74*). Vaginal plugs were checked the next morning, and were referred to as embryonic day 0.5

(E0.5). Mice were taken at different time-points as indicated in text, adult mice cortex, hippocampus, and spinal cords were taken at age of 8 weeks. Pre-natal brain were dissected and stripped of meninges. Adult and post-natal mice were perfused with PBS transcardially; brains were dissected and stripped of meninges and choroid plexus. Single-cell suspensions were achieved using software-controlled sealed homogenization system (Dispomix; http://www.biocellisolation.com) in PBS, followed by density gradient separation; Pellet was mixed with 40% percoll and centrifuged in 800G for 20 min at room temperature. Supernatant was discarded and pellet taken further for antibody staining. Samples were first blocked with Fc-block CD16/32 (BD Biosciences, San Jose, CA) at gated for $CD45^{int}$ (1:150, 30-F11, biolegend Inc.), $CD11b^{int}$ (1:150, M1/70, biolegend Inc.), and $CX3CR1\text{-}GFP^{+}$. Cell populations were sorted with SORP-aria (BD Biosciences, San Jose, CA).

Germ-free mice

Wild-type C57/Bl6 mice were born and raised in sterile isolators in the absence of any microbial colonization as described previously (*75*). Sterility was routinely monitored by PCR- and culture-based methods. Brains from GF mice and SPF controls were taken at day 1 and week 4. Microglia from whole brains was harvested as described above and gated for $CD45^{int}$ and $CD11b^{int}$, as we and others have carefully confirmed these cells to be similar to the populations collected from the CX3CR1-GFP+ microglia populations (see fig. S1C). Cell populations were sorted with SORP-aria (BD Biosciences, San Jose, CA).

Maternal immune activation by poly I:C

Naïve female mice were bred overnight with C57BL/6J males. Vaginal plugs were checked the next morning, and were referred to as embryonic day 0.5 (E0.5). On E12.5 or E14.5, pregnant females were injected intravenously (i.v.) with a single dose of 5 mg/kg poly I:C (Sigma-Aldrich, Rehovot, Israel) dissolved in PBS, or an equivalent volume of PBS as a control. The dose of poly I:C was determined according to Meyer *et al.* 2007 (*76*). The injection volume was 5 ml/kg. Pups from injected animals were taken at postnatal day one and at age of 4 weeks. Microglia was harvested from whole brains as described above, and gated by $CD45^{int}$ and $CD11b^{int}$, as we and others have carefully confirmed these cells to be similar to the populations collected from the CX3CR1-GFP+ microglia populations (see fig. S1C). Cell populations were sorted with SORP-aria (BD Biosciences, San Jose, CA).

MafB knockout mice

Female $MafB^{fl/+}Csf1R\text{-}Cre^{-/-}$ or $MafB^{fl/fl}Csf1R\text{-}Cre^{-/-}$ were bred with male $MafB^{fl/fl}Csf1R\text{-}Cre^{+/-}$ (Refer to supplementary materials for description of knockout generation). Vaginal plugs were checked the next morning, and were referred to as embryonic day 0.5 (E0.5). Post-natal mice were taken at P2 and adults at age of 5 weeks, animals were perfused with PBS transcardially; brains were dissected and stripped of meninges and choroid plexus. Microglia was harvested from whole brains. Single cell suspension was achieved by mechanical dissociation, followed by density gradient separation; Pellet was mixed with 70% percoll and overlayed on 37% percoll underlayed by 30% percoll, centrifuged in 800G for 30 min at 4°C. 37%/70% interface was collected for antibody staining. Samples were) pre-gated using Zombie Violet fixable viability kit (Biolegend, France) and $Ly6C^{-}$ (HK1.4, Biolegend, France) then gated for $CD45.2^{int}$ (104, BD biosciences, France), $CD11b^{int}$ (1:150, M1/70, BD biosciences, Francebiolegend Inc.), Cell populations were sorted with SORP-ariaBD FACSAria III (BD Biosciences, San Jose, CAFrance).

Single-molecule fluorescent in situ hybridization (smFISH)

$CX3CR1^{GFP/+}$ were perfused, Brain tissues harvested and fixed in 4% paraformaldehyde for 3 hours; incubated overnight with 30% sucrose in 4% paraformaldehyde and then embedded in OCT. 7 μm cryosections were used for hybridization. Probe libraries were designed and constructed as previously described (*53*). Single molecule FISH probe libraries consisted of 48 probes of length 20 bps, and were coupled to cy5 or alexa594. Hybridizations were performed overnight in 30°C. DAPI dye for nuclear staining was added during the washes. To detect microglia, $CX3CR1^{GFP/+}$ mice were used and cells were detected by their GFP fluorescent signal. Images were taken with a Nikon Ti-E inverted fluorescence microscope equipped with a ×100 oil-immersion objective and a Photometrics Pixis 1024 CCD camera using MetaMorph software (Molecular Devices, Downington, PA). The image-plane pixel dimension was 0.13 μm. P-values were calculated by Fisher exact test. (*77*)

RNA sequencing

Cells were harvested at different time points into Lysis/Binding buffer (Invitrogen). mRNA was captured with 12 μl of Dynabeads oli-go(dT) (Life Technologies), washed, and eluted at 70°C with 10 μl of 10 mM Tris-Cl (pH 7.5). RNA-seq was performed using as previously described (*50*) and DNA libraries were sequenced on an Illumina NextSEq. 500 or HiSeq with an average of 4 million aligned reads per sample.

RNA processing and analysis

We aligned the RNA-seq reads to the mouse reference genome (NCBI 37, mm9) using TopHat v2.0.13 with default

parameters (*78*). Duplicate reads were filtered if they aligned to the same base and had identical UMIs. Expression levels were calculated and normalized for each sample to the total number of reads using HOMER software (http://homer.salk.edu) with the command "*analyzeRepeats.pl rna mm9 -d [sample files] -count 3utr -condenseGenes*" (*79*). For the RNA-seq analysis in Fig. 1, we focused on highly expressed genes with 2-fold differential over the noise (set at 100) between the means of at least two time points (3059 genes). The value of *k* for the K-means clustering (matlab function *kmeans*) was chosen by assessing the average silhouette (matlab function *evalclusters*; higher score means more cohesive clusters) for a range of possible values with correlation as the distance metric (fig. S1C). GO associations for each cluster were determined using GOrilla http://cbl-gorilla.cs.technion.ac.il/ (*80*, *81*). The overlap with microglia-specific genes was determined by comparison with genes from the brain-specific macrophage expression cluster in (*16*) and the significance of enrichment was calculated using a Hypergeometric distribution. The subset of genes that were differential across CNS regions was determined based on a greater than 2-fold differential between any two of the three regions (cortex, hippocampus, and spinal cord) and the highest expression of the three falling within 2-fold of the maximum expression across microglia development. NMF and PCA were performed using built-in matlab function *nnmf* and *pca*, respectively. The value of *k* for the NMF was chosen by assessing the plot of root mean square residuals for a range of values (fig. S1F).

iChIP

Naïve C57BL/6J female mice were bred overnight with $CX3CR1^{GFP/GFP}$ males (*74*). Vaginal plugs were checked the next morning, and were referred to as embryonic day 0.5 (E0.5). Mice were taken at E12.5, day 1, and 8 weeks. Microglia was harvested from whole brains and sorted as indicated above. iChIP was prepared as previously described (*47*).

ATAC-seq

Naïve C57BL/6J female mice were bred overnight with $CX3CR1^{GFP/GFP}$ males (*74*). Vaginal plugs were checked the next morning, and were referred to as embryonic day 0.5 (E0.5). Mice were taken at E12.5, day 3, and 8 weeks. Microglia was harvested from whole brains and sorted as indicated above. To profile for open chromatin, we used an adaptation of Assay for Transposase Accessible Chromatin (ATAC-seq) protocol (*46*, *82*) as previously described (*16*).

Processing of ChIP-seq and ATAC-seq

Reads were aligned to the mouse reference genome (mm9, NCBI 37) using Bowtie2 aligner version 2.2.5 (*83*) with default parameters. The Picard tool *MarkDuplicates* from the Broad Institute (http://broadinstitute.github.io/picard/) was used to remove PCR duplicates. To identify regions of enrichment (peaks) from ChIP-seq reads of H3K4me2 and ATAC-seq, we used the HOMER package *makeTagDirectory* followed by *findPeaks* command with the histone parameter or 500bp centered regions, respectively (*79*). Union peaks file were generated for ATAC by combining and merging overlapping peaks in all samples.

Chromatin analysis

The read density (number of reads in 10 million total reads per 1000 bp) for H3K4me2 and ATAC was calculated in each region from the union ATAC peaks files. We consider promoters to be within +/− 2000bp of a TSS (n=12930). We defined 11252 high confidence distal enhancers based on their presence in at least two replicates of the same ATAC-seq population, the distal location of the regions (i.e., excluding promoters), and the average K4me2 read density. The region intensity was given in log-base2 of the normalized density (log2(x+1)). The value of *k* for the K-means clustering (matlab function *kmeans*) was chosen by assessing the average silhouette (matlab function *evalclusters*) for a range of possible values with correlation as the distance metric (fig. S3D). The significance of the overlap between chromatin categories and expression clusters was determined using the hypergeometric distribution ($p<0.05$; table S4).

Gene tracks and normalization

All gene tracks were visualized as *bigWig* files of the combined replicates normalized to 10,000,000 reads and created by the HOMER algorithm *makeUCSCfile (79)*. For visualization, the tracks were smoothed by averaging over a sliding window of 500 bases and all tracks for a given region were scaled to the highest overall peak.

Single cell sorting

Naïve C57BL/6J female mice were bred overnight with $CX3CR1^{GFP/GFP}$ males (*74*). Vaginal plugs were checked the next morning, and were referred to as embryonic day 0.5 (E0.5). Mice were taken at E12.5, E18.5, and 8 weeks. Microglia was harvested and sorted from whole brains as indicated above.into 384-well cell capture plates containing 2 μl of lysis solution and barcoded poly(T) reverse-transcription (RT) primers for single-cell RNA-seq (*50*). Barcoded single cell capture plates were prepared with a Bravo automated liquid handling platform (Agilent) as described previously (*50*). Four empty wells were kept in each 384-well plate as a no-cell control during data analysis. Immediately after sorting, each plate was spun down to ensure cell immersion into the lysis solution, snap frozen on dry ice and stored at -80°C until processed.

Single cell libraries and analysis

Single cell libraries were prepared using the MARS-seq protocol and processed as described previously (*50*). In order to assess the heterogeneity of the previously-defined phases in microglia development, we used a recently published batch-aware multinomial mixture-model clustering algorithm (*51*). Since samples derive from different spatial and temporal points, we devised an approach that would reduce batch effect within each sample but preserve genuine gene expression differences between samples. Each sample, consisting of four batches, was clustered separately. This preliminary clustering was used to infer optimum batch correction coefficients for each gene. A new debatched UMI dataset was created, implementing the inferred corrections on the UMI count. The debatched dataset was then used to jointly cluster all samples using the same algorithm with no debatching (all batch correction coefficients were set to 1).

This two-steps clustering approach proved to increase likelihood score and significantly reduce intra-cluster gene variance when compared to clustering each sample separately, allowing debatching between samples or disallowing debatching completely.

Immunohistochemistry

Mice were transcardially perfused with PBS prior to brain tissue fixation. The following primary antibodies were used: mouse anti-Dab2 (1:100; BD bioscience, San Jose, CA), Rabbit anti-GFP (1:100, MBL, Woburn, MA), Goat anti-GFP (1:100; abcam, Cambridge, MA), Goat anti-IBA1 (1:100, abcam, Cambridge, MA), Rabbit anti-MafB (1:100, Bethyl Laboratories, Inc., Montgomery, TX). Secondary antibodies were Cy3/Cy2 conjugated donkey anti-mouse/goat antibodies (1:200; Jackson ImmunoResearch, West Grove, PA). The slides were exposed to Hoechst nuclear staining (1:4000; Invitrogen Probes, Carlsbad, CA) for 1 min, prior to their sealing. Two negative controls were used in immunostaining procedures: staining with isotype control antibody followed by secondary antibody, or staining with secondary antibody alone.

For Dab2 staining, microglia from CX3CR1$^{GFP/+}$ mice underwent tissue processing and immunohistochemistry on paraffin embedded sectioned (6 μm thick). Microscopic analysis was performed using a fluorescence microscope (E800; Nikon).

For MafB staining, microglia from wild-type mice underwent tissue processing and immunohistochemistry on floating sections (30 μm thick). Microscopic analysis was performed using confocal microscopy (Zeiss, LSM880).

Motif analysis

For motif finding, we used the sets of genes from each expression cluster (Fig. 1C) individually as input for HOMER package motif finder algorithm *findMotifGenome.pl* (*79*). By parsing the known motif list, we compiled the occurrences of the sequence motifs for the transcription factors of interest within the promoters of each expression cluster. A hypergeometric distribution was used to calculate the significance of the overlap between motif occurrences in our set and the expression clusters from Fig. 1C.

Statistical methods

In general, two replicates (in some cases, averaged over offspring from same mother) per sample from independent mice were used for the analyses, so that comparisons between time points would be comparable. In the poly I:C experiment, replicates originated from different mothers. The MafB knockout experiment used 3 replicates from independent mice for both newborn and adult. Genes were considered to have increased or decreased in expression if the log fold change was greater than 1 between the mean of replicates. Genes with normalized log expression value less than 6 were not used for this comparison because of the noise at these low expression levels. P values for expression changes used in the volcano plots were calculated using two-tailed *t* test on the log expression values. A hypergeometric distribution was used to calculate the significance of the overlap between differentially expressed genes, motifs, chromatin clusters, and the expression clusters from Fig. 1C. GO associations and related P-values were determined using GOrilla http://cbl-gorilla.cs.technion.ac.il/ (*80*, *81*). Pairwise similarity between replicates or samples was given as the Pearson's correlation.

For further details, please refer to the supplementary materials.

REFERENCES AND NOTES

1. U.-K. Hanisch, H. Kettenmann, Microglia: Active sensor and versatile effector cells in the normal and pathologic brain. *Nat. Neurosci.* **10**, 1387–1394 (2007). Medline doi:10.1038/nn1997
2. A. Nimmerjahn, F. Kirchhoff, F. Helmchen, Resting microglial cells are highly dynamic surveillants of brain parenchyma in vivo. *Science* **308**, 1314–1318 (2005). Medline doi:10.1126/science.1110647
3. M. Prinz, J. Priller, S. S. Sisodia, R. M. Ransohoff, Heterogeneity of CNS myeloid cells and their roles in neurodegeneration. *Nat. Neurosci.* **14**, 1227–1235 (2011). Medline doi:10.1038/nn.2923
4. E. Gomez Perdiguero, K. Klapproth, C. Schulz, K. Busch, E. Azzoni, L. Crozet, H. Garner, C. Trouillet, M. F. de Bruijn, F. Geissmann, H. R. Rodewald, Tissue-resident macrophages originate from yolk-sac-derived erythro-myeloid progenitors. *Nature* **518**, 547–551 (2015). Medline doi:10.1038/nature13989
5. F. Ginhoux, M. Greter, M. Leboeuf, S. Nandi, P. See, S. Gokhan, M. F. Mehler, S. J. Conway, L. G. Ng, E. R. Stanley, I. M. Samokhvalov, M. Merad, Fate mapping analysis reveals that adult microglia derive from primitive macrophages. *Science* **330**, 841–845 (2010). Medline doi:10.1126/science.1194637
6. C. Schulz, E. Gomez Perdiguero, L. Chorro, H. Szabo-Rogers, N. Cagnard, K. Kierdorf, M. Prinz, B. Wu, S. E. Jacobsen, J. W. Pollard, J. Frampton, K. J. Liu, F. Geissmann, A lineage of myeloid cells independent of Myb and hematopoietic stem cells. *Science* **336**, 86–90 (2012). Medline doi:10.1126/science.1219179
7. K. Kierdorf, D. Erny, T. Goldmann, V. Sander, C. Schulz, E. G. Perdiguero, P.

Wieghofer, A. Heinrich, P. Riemke, C. Hölscher, D. N. Müller, B. Luckow, T. Brocker, K. Debowski, G. Fritz, G. Opdenakker, A. Diefenbach, K. Biber, M. Heikenwalder, F. Geissmann, F. Rosenbauer, M. Prinz, Microglia emerge from erythromyeloid precursors via Pu.1- and Irf8-dependent pathways. *Nat. Neurosci.* **16**, 273–280 (2013). Medline

8. J. Bruttger, K. Karram, S. Wörtge, T. Regen, F. Marini, N. Hoppmann, M. Klein, T. Blank, S. Yona, Y. Wolf, M. Mack, E. Pinteaux, W. Müller, F. Zipp, H. Binder, T. Bopp, M. Prinz, S. Jung, A. Waisman, Genetic cell ablation reveals clusters of local self-renewing microglia in the mammalian central nervous system. *Immunity* **43**, 92–106 (2015). Medline doi:10.1016/j.immuni.2015.06.012
9. B. Ajami, J. L. Bennett, C. Krieger, W. Tetzlaff, F. M. V. Rossi, Local self-renewal can sustain CNS microglia maintenance and function throughout adult life. *Nat. Neurosci.* **10**, 1538–1543 (2007). Medline doi:10.1038/nn2014
10. D. Hashimoto, A. Chow, C. Noizat, P. Teo, M. B. Beasley, M. Leboeuf, C. D. Becker, P. See, J. Price, D. Lucas, M. Greter, A. Mortha, S. W. Boyer, E. C. Forsberg, M. Tanaka, N. van Rooijen, A. García-Sastre, E. R. Stanley, F. Ginhoux, P. S. Frenette, M. Merad, Tissue-resident macrophages self-maintain locally throughout adult life with minimal contribution from circulating monocytes. *Immunity* **38**, 792–804 (2013). Medline doi:10.1016/j.immuni.2013.04.004
11. J. Sheng, C. Ruedl, K. Karjalainen, Most tissue-resident macrophages except microglia are derived from fetal hematopoietic stem cells. *Immunity* **43**, 382–393 (2015). Medline doi:10.1016/j.immuni.2015.07.016
12. A. Mildner, H. Schmidt, M. Nitsche, D. Merkler, U. K. Hanisch, M. Mack, M. Heikenwalder, W. Brück, J. Priller, M. Prinz, Microglia in the adult brain arise from Ly-6C^{hi}CCR2^{+} monocytes only under defined host conditions. *Nat. Neurosci.* **10**, 1544–1553 (2007). Medline doi:10.1038/nn2015
13. R. Shechter, A. London, C. Varol, C. Raposo, M. Cusimano, G. Yovel, A. Rolls, M. Mack, S. Pluchino, G. Martino, S. Jung, M. Schwartz, Infiltrating blood-derived macrophages are vital cells playing an anti-inflammatory role in recovery from spinal cord injury in mice. *PLOS Med.* **6**, e1000113 (2009). Medline doi:10.1371/journal.pmed.1000113
14. R. Shechter, O. Miller, G. Yovel, N. Rosenzweig, A. London, J. Ruckh, K. W. Kim, E. Klein, V. Kalchenko, P. Bendel, S. A. Lira, S. Jung, M. Schwartz, Recruitment of beneficial M2 macrophages to injured spinal cord is orchestrated by remote brain choroid plexus. *Immunity* **38**, 555–569 (2013). Medline
15. D. Gosselin, V. M. Link, C. E. Romanoski, G. J. Fonseca, D. Z. Eichenfield, N. J. Spann, J. D. Stender, H. B. Chun, H. Garner, F. Geissmann, C. K. Glass, Environment drives selection and function of enhancers controlling tissue-specific macrophage identities. *Cell* **159**, 1327–1340 (2014). Medline doi:10.1016/j.cell.2014.11.023
16. Y. Lavin, D. Winter, R. Blecher-Gonen, E. David, H. Keren-Shaul, M. Merad, S. Jung, I. Amit, Tissue-resident macrophage enhancer landscapes are shaped by the local microenvironment. *Cell* **159**, 1312–1326 (2014). Medline doi:10.1016/j.cell.2014.11.018
17. M. Greter, I. Lelios, P. Pelczar, G. Hoeffel, J. Price, M. Leboeuf, T. M. Kündig, K. Frei, F. Ginhoux, M. Merad, B. Becher, Stroma-derived interleukin-34 controls the development and maintenance of Langerhans cells and the maintenance of microglia. *Immunity* **37**, 1050–1060 (2012). Medline doi:10.1016/j.immuni.2012.11.001
18. Y. Wang, K. J. Szretter, W. Vermi, S. Gilfillan, C. Rossini, M. Cella, A. D. Barrow, M. S. Diamond, M. Colonna, IL-34 is a tissue-restricted ligand of CSF1R required for the development of Langerhans cells and microglia. *Nat. Immunol.* **13**, 753–760 (2012). Medline doi:10.1038/ni.2360
19. O. Butovsky, M. P. Jedrychowski, C. S. Moore, R. Cialic, A. J. Lanser, G. Gabriely, T. Koeglsperger, B. Dake, P. M. Wu, C. E. Doykan, Z. Fanek, L. Liu, Z. Chen, J. D. Rothstein, R. M. Ransohoff, S. P. Gygi, J. P. Antel, H. L. Weiner, Identification of a unique TGF-β–dependent molecular and functional signature in microglia. *Nat. Neurosci.* **17**, 131–143 (2014). Medline doi:10.1038/nn.3599
20. M. Cohen, O. Matcovitch, E. David, Z. Barnett-Itzhaki, H. Keren-Shaul, R. Blecher-Gonen, D. A. Jaitin, A. Sica, I. Amit, M. Schwartz, Chronic exposure to TGFβ1 regulates myeloid cell inflammatory response in an IRF7-dependent manner. *EMBO J.* **33**, 2906–2921 (2014). Medline doi:10.15252/embj.201489293
21. D. Erny, A. L. Hrabě de Angelis, D. Jaitin, P. Wieghofer, O. Staszewski, E. David, H. Keren-Shaul, T. Mahlakoiv, K. Jakobshagen, T. Buch, V. Schwierzeck, O. Utermöhlen, E. Chun, W. S. Garrett, K. D. McCoy, A. Diefenbach, P. Staeheli, B. Stecher, I. Amit, M. Prinz, Host microbiota constantly control maturation and function of microglia in the CNS. *Nat. Neurosci.* **18**, 965–977 (2015). Medline doi:10.1038/nn.4030
22. S. Sawa, M. Lochner, N. Satoh-Takayama, S. Dulauroy, M. Bérard, M. Kleinschek, D. Cua, J. P. Di Santo, G. Eberl, RORγt^{+} innate lymphoid cells regulate intestinal homeostasis by integrating negative signals from the symbiotic microbiota. *Nat. Immunol.* **12**, 320–326 (2011). Medline doi:10.1038/ni.2002
23. P. H. Patterson, Immune involvement in schizophrenia and autism: Etiology, pathology and animal models. *Behav. Brain Res.* **204**, 313–321 (2009). Medline doi:10.1016/j.bbr.2008.12.016
24. G. Hoeffel, J. Chen, Y. Lavin, D. Low, F. F. Almeida, P. See, A. E. Beaudin, J. Lum, I. Low, E. C. Forsberg, M. Poidinger, F. Zolezzi, A. Larbi, L. G. Ng, J. K. Chan, M. Greter, B. Becher, I. M. Samokhvalov, M. Merad, F. Ginhoux, C-Myb^{+} erythro-myeloid progenitor-derived fetal monocytes give rise to adult tissue-resident macrophages. *Immunity* **42**, 665–678 (2015). Medline doi:10.1016/j.immuni.2015.03.011
25. S. Wakselman, C. Béchade, A. Roumier, D. Bernard, A. Triller, A. Bessis, Developmental neuronal death in hippocampus requires the microglial CD11b integrin and DAP12 immunoreceptor. *J. Neurosci.* **28**, 8138–8143 (2008). Medline doi:10.1523/JNEUROSCI.1006-08.2008
26. A. Sierra, J. M. Encinas, J. J. Deudero, J. H. Chancey, G. Enikolopov, L. S. Overstreet-Wadiche, S. E. Tsirka, M. Maletic-Savatic, Microglia shape adult hippocampal neurogenesis through apoptosis-coupled phagocytosis. *Cell Stem Cell* **7**, 483–495 (2010). Medline doi:10.1016/j.stem.2010.08.014
27. R. C. Paolicelli, G. Bolasco, F. Pagani, L. Maggi, M. Scianni, P. Panzanelli, M. Giustetto, T. A. Ferreira, E. Guiducci, L. Dumas, D. Ragozzino, C. T. Gross, Synaptic pruning by microglia is necessary for normal brain development. *Science* **333**, 1456–1458 (2011). Medline doi:10.1126/science.1202529
28. D. P. Schafer, E. K. Lehrman, A. G. Kautzman, R. Koyama, A. R. Mardinly, R. Yamasaki, R. M. Ransohoff, M. E. Greenberg, B. A. Barres, B. Stevens, Microglia sculpt postnatal neural circuits in an activity and complement-dependent manner. *Neuron* **74**, 691–705 (2012). Medline doi:10.1016/j.neuron.2012.03.026
29. D. P. Schafer, E. K. Lehrman, B. Stevens, The "quad-partite" synapse: Microglia-synapse interactions in the developing and mature CNS. *Glia* **61**, 24–36 (2013). Medline doi:10.1002/glia.22389
30. H. Kettenmann, F. Kirchhoff, A. Verkhratsky, Microglia: New roles for the synaptic stripper. *Neuron* **77**, 10–18 (2013). Medline doi:10.1016/j.neuron.2012.12.023
31. Y. Zhan, R. C. Paolicelli, F. Sforazzini, L. Weinhard, G. Bolasco, F. Pagani, A. L. Vyssotski, A. Bifone, A. Gozzi, D. Ragozzino, C. T. Gross, Deficient neuron-microglia signaling results in impaired functional brain connectivity and social behavior. *Nat. Neurosci.* **17**, 400–406 (2014). Medline doi:10.1038/nn.3641
32. A. S. Brown, E. J. Derkits, Prenatal infection and schizophrenia: A review of epidemiologic and translational studies. *Am. J. Psychiatry* **167**, 261–280 (2010). Medline doi:10.1176/appi.ajp.2009.09030361
33. K. A. Garbett, E. Y. Hsiao, S. Kálmán, P. H. Patterson, K. Mirnics, Effects of maternal immune activation on gene expression patterns in the fetal brain. *Transl. Psychiatry* **2**, e98 (2012). Medline doi:10.1038/tp.2012.24
34. U. Meyer, J. Feldon, M. Schedlowski, B. K. Yee, Immunological stress at the maternal-foetal interface: A link between neurodevelopment and adult psychopathology. *Brain Behav. Immun.* **20**, 378–388 (2006). Medline doi:10.1016/j.bbi.2005.11.003
35. U. Meyer, M. Nyffeler, A. Engler, A. Urwyler, M. Schedlowski, I. Knuesel, B. K. Yee, J. Feldon, The time of prenatal immune challenge determines the specificity of inflammation-mediated brain and behavioral pathology. *J. Neurosci.* **26**, 4752–4762 (2006). Medline doi:10.1523/JNEUROSCI.0099-06.2006
36. D. Gate, K. Rezai-Zadeh, D. Jodry, A. Rentsendorj, T. Town, Macrophages in Alzheimer's disease: The blood-borne identity. *J Neural Transm.* **117**, 961–970 (2010). Medline doi:10.1007/s00702-010-0422-7
37. C. Prunier, P. H. Howe, Disabled-2 (Dab2) is required for transforming growth factor β-induced epithelial to mesenchymal transition (EMT). *J. Biol. Chem.* **280**, 17540–17548 (2005). Medline doi:10.1074/jbc.M500974200
38. Materials and methods are available as supplementary materials on *Science* Online.
39. G. Brady, F. Billia, J. Knox, T. Hoang, I. R. Kirsch, E. B. Voura, R. G. Hawley, R.

Cumming, M. Buchwald, K. Siminovitch, N. Miyamoto, G. Boehmelt, N. N. Iscove, Analysis of gene expression in a complex differentiation hierarchy by global amplification of cDNA from single cells. *Curr. Biol.* **5**, 909–922 (1995). Medline doi:10.1016/S0960-9822(95)00181-3
40. S. D. J. Calaminus, A. V. Guitart, A. Sinclair, H. Schachtner, S. P. Watson, T. L. Holyoake, K. R. Kranc, L. M. Machesky, Lineage tracing of Pf4-Cre marks hematopoietic stem cells and their progeny. *PLOS ONE* **7**, e51361 (2012). Medline doi:10.1371/journal.pone.0051361
41. I. Amit, D. R. Winter, S. Jung, The role of the local environment and epigenetics in shaping macrophage identity and their effect on tissue homeostasis. *Nat. Immunol.* **17**, 18–25 (2016). Medline doi:10.1038/ni.3325
42. D. D. Lee, H. S. Seung, Learning the parts of objects by non-negative matrix factorization. *Nature* **401**, 788–791 (1999). Medline doi:10.1038/44565
43. D. S. Gross, W. T. Garrard, Nuclease hypersensitive sites in chromatin. *Annu. Rev. Biochem.* **57**, 159–197 (1988). Medline doi:10.1146/annurev.bi.57.070188.001111
44. G. Felsenfeld, M. Groudine, Controlling the double helix. *Nature* **421**, 448–453 (2003). Medline doi:10.1038/nature01411
45. D. R. Winter, I. Amit, The role of chromatin dynamics in immune cell development. *Immunol. Rev.* **261**, 9–22 (2014). Medline doi:10.1111/imr.12200
46. J. D. Buenrostro, P. G. Giresi, L. C. Zaba, H. Y. Chang, W. J. Greenleaf, Transposition of native chromatin for fast and sensitive epigenomic profiling of open chromatin, DNA-binding proteins and nucleosome position. *Nat. Methods* **10**, 1213–1218 (2013). Medline doi:10.1038/nmeth.2688
47. D. Lara-Astiaso, A. Weiner, E. Lorenzo-Vivas, I. Zaretsky, D. A. Jaitin, E. David, H. Keren-Shaul, A. Mildner, D. Winter, S. Jung, N. Friedman, I. Amit, Chromatin state dynamics during blood formation. *Science* **345**, 943–949 (2014). Medline doi:10.1126/science.1256271
48. A. Barski, S. Cuddapah, K. Cui, T. Y. Roh, D. E. Schones, Z. Wang, G. Wei, I. Chepelev, K. Zhao, High-resolution profiling of histone methylations in the human genome. *Cell* **129**, 823–837 (2007). Medline doi:10.1016/j.cell.2007.05.009
49. N. D. Heintzman, R. K. Stuart, G. Hon, Y. Fu, C. W. Ching, R. D. Hawkins, L. O. Barrera, S. Van Calcar, C. Qu, K. A. Ching, W. Wang, Z. Weng, R. D. Green, G. E. Crawford, B. Ren, Distinct and predictive chromatin signatures of transcriptional promoters and enhancers in the human genome. *Nat. Genet.* **39**, 311–318 (2007). Medline doi:10.1038/ng1966
50. D. A. Jaitin, E. Kenigsberg, H. Keren-Shaul, N. Elefant, F. Paul, I. Zaretsky, A. Mildner, N. Cohen, S. Jung, A. Tanay, I. Amit, Massively parallel single-cell RNA-seq for marker-free decomposition of tissues into cell types. *Science* **343**, 776–779 (2014). Medline doi:10.1126/science.1247651
51. F. Paul, Y. Arkin, A. Giladi, D. A. Jaitin, E. Kenigsberg, H. Keren-Shaul, D. Winter, D. Lara-Astiaso, M. Gury, A. Weiner, E. David, N. Cohen, F. K. Lauridsen, S. Haas, A. Schlitzer, A. Mildner, F. Ginhoux, S. Jung, A. Trumpp, B. T. Porse, A. Tanay, I. Amit, Transcriptional heterogeneity and lineage commitment in myeloid progenitors. *Cell* **163**, 1663–1677 (2015). Medline doi:10.1016/j.cell.2015.11.013
52. K. Bahar Halpern, S. Tanami, S. Landen, M. Chapal, L. Szlak, A. Hutzler, A. Nizhberg, S. Itzkovitz, Bursty gene expression in the intact mammalian liver. *Mol. Cell* **58**, 147–156 (2015). Medline doi:10.1016/j.molcel.2015.01.027
53. S. Itzkovitz, I. C. Blat, T. Jacks, H. Clevers, A. van Oudenaarden, Optimality in the development of intestinal crypts. *Cell* **148**, 608–619 (2012). Medline doi:10.1016/j.cell.2011.12.025
54. A. Lyubimova, S. Itzkovitz, J. P. Junker, Z. P. Fan, X. Wu, A. van Oudenaarden, Single-molecule mRNA detection and counting in mammalian tissue. *Nat. Protoc.* **8**, 1743–1758 (2013). Medline doi:10.1038/nprot.2013.109
55. E. S. Lein, M. J. Hawrylycz, N. Ao, M. Ayres, A. Bensinger, A. Bernard, A. F. Boe, M. S. Boguski, K. S. Brockway, E. J. Byrnes, L. Chen, L. Chen, T.-M. Chen, M. Chi Chin, J. Chong, B. E. Crook, A. Czaplinska, C. N. Dang, S. Datta, N. R. Dee, A. L. Desaki, T. Desta, E. Diep, T. A. Dolbeare, M. J. Donelan, H.-W. Dong, J. G. Dougherty, B. J. Duncan, A. J. Ebbert, G. Eichele, L. K. Estin, C. Faber, B. A. Facer, R. Fields, S. R. Fischer, T. P. Fliss, C. Frensley, S. N. Gates, K. J. Glattfelder, K. R. Halverson, M. R. Hart, J. G. Hohmann, M. P. Howell, D. P. Jeung, R. A. Johnson, P. T. Karr, R. Kawal, J. M. Kidney, R. H. Knapik, C. L. Kuan, J. H. Lake, A. R. Laramee, K. D. Larsen, C. Lau, T. A. Lemon, A. J. Liang, Y. Liu, L. T. Luong, J. Michaels, J. J. Morgan, R. J. Morgan, M. T. Mortrud, N. F. Mosqueda, L. L. Ng, R. Ng, G. J. Orta, C. C. Overly, T. H. Pak, S. E. Parry, S. D. Pathak, O. C. Pearson, R. B. Puchalski, Z. L. Riley, H. R. Rockett, S. A. Rowland, J. J. Royall, M. J. Ruiz, N. R. Sarno, K. Schaffnit, N. V. Shapovalova, T. Sivisay, C. R. Slaughterbeck, S. C. Smith, K. A. Smith, B. I. Smith, A. J. Sodt, N. N. Stewart, K.-R. Stumpf, S. M. Sunkin, M. Sutram, A. Tam, C. D. Teemer, C. Thaller, C. L. Thompson, L. R. Varnam, A. Visel, R. M. Whitlock, P. E. Wohnoutka, C. K. Wolkey, V. Y. Wong, M. Wood, M. B. Yaylaoglu, R. C. Young, B. L. Youngstrom, X. Feng Yuan, B. Zhang, T. A. Zwingman, A. R. Jones, Genome-wide atlas of gene expression in the adult mouse brain. *Nature* **445**, 168–176 (2007). Medline doi:10.1038/nature05453
56. L. A. Cirillo, K. S. Zaret, An early developmental transcription factor complex that is more stable on nucleosome core particles than on free DNA. *Mol. Cell* **4**, 961–969 (1999). Medline doi:10.1016/S1097-2765(00)80225-7
57. M. Garber, N. Yosef, A. Goren, R. Raychowdhury, A. Thielke, M. Guttman, J. Robinson, B. Minie, N. Chevrier, Z. Itzhaki, R. Blecher-Gonen, C. Bornstein, D. Amann-Zalcenstein, A. Weiner, D. Friedrich, J. Meldrim, O. Ram, C. Cheng, A. Gnirke, S. Fisher, N. Friedman, B. Wong, B. E. Bernstein, C. Nusbaum, N. Hacohen, A. Regev, I. Amit, A high-throughput chromatin immunoprecipitation approach reveals principles of dynamic gene regulation in mammals. *Mol. Cell* **47**, 810–822 (2012). Medline doi:10.1016/j.molcel.2012.07.030
58. A. Aziz, E. Soucie, S. Sarrazin, M. H. Sieweke, MafB/c-Maf deficiency enables self-renewal of differentiated functional macrophages. *Science* **326**, 867–871 (2009). Medline doi:10.1126/science.1176056
59. L. M. Kelly, U. Englmeier, I. Lafon, M. H. Sieweke, T. Graf, MafB is an inducer of monocytic differentiation. *EMBO J.* **19**, 1987–1997 (2000). Medline doi:10.1093/emboj/19.9.1987
60. E. L. Soucie, Z. Weng, L. Geirsdóttir, K. Molawi, J. Maurizio, R. Fenouil, N. Mossadegh-Keller, G. Gimenez, L. VanHille, M. Beniazza, J. Favret, C. Berruyer, P. Perrin, N. Hacohen, J. C. Andrau, P. Ferrier, P. Dubreuil, A. Sidow, M. H. Sieweke, Lineage-specific enhancers activate self-renewal genes in macrophages and embryonic stem cells. *Science* **351**, aad5510 (2016). Medline doi:10.1126/science.aad5510
61. E. Y. Hsiao, S. W. McBride, S. Hsien, G. Sharon, E. R. Hyde, T. McCue, J. A. Codelli, J. Chow, S. E. Reisman, J. F. Petrosino, P. H. Patterson, S. K. Mazmanian, Microbiota modulate behavioral and physiological abnormalities associated with neurodevelopmental disorders. *Cell* **155**, 1451–1463 (2013). Medline doi:10.1016/j.cell.2013.11.024
62. L. V. Hooper, D. R. Littman, A. J. Macpherson, Interactions between the microbiota and the immune system. *Science* **336**, 1268–1273 (2012). Medline doi:10.1126/science.1223490
63. J. E. Koenig, A. Spor, N. Scalfone, A. D. Fricker, J. Stombaugh, R. Knight, L. T. Angenent, R. E. Ley, Succession of microbial consortia in the developing infant gut microbiome. *Proc. Natl. Acad. Sci. U.S.A.* **108**, 4578–4585 (2011). Medline doi:10.1073/pnas.1000081107
64. M.-C. Arrieta, L. T. Stiemsma, N. Amenyogbe, E. M. Brown, B. Finlay, The intestinal microbiome in early life: Health and disease. *Front. Immunol.* **5**, 427 (2014). Medline
65. P. H. Patterson, Maternal infection and immune involvement in autism. *Trends Mol. Med.* **17**, 389–394 (2011). Medline doi:10.1016/j.molmed.2011.03.001
66. S. Giovanoli, U. Weber-Stadlbauer, M. Schedlowski, U. Meyer, H. Engler, Prenatal immune activation causes hippocampal synaptic deficits in the absence of overt microglia anomalies. *Brain Behav. Immun.* **55**, 25–38 (2015). Medline
67. S. Yona, K. W. Kim, Y. Wolf, A. Mildner, D. Varol, M. Breker, D. Strauss-Ayali, S. Viukov, M. Guilliams, A. Misharin, D. A. Hume, H. Perlman, B. Malissen, E. Zelzer, S. Jung, Fate mapping reveals origins and dynamics of monocytes and tissue macrophages under homeostasis. *Immunity* **38**, 79–91 (2013). Medline doi:10.1016/j.immuni.2012.12.001
68. I. G. Pantoja-Feliciano, J. C. Clemente, E. K. Costello, M. E. Perez, M. J. Blaser, R. Knight, M. G. Dominguez-Bello, Biphasic assembly of the murine intestinal microbiota during early development. *ISME J.* **7**, 1112–1115 (2013). Medline doi:10.1038/ismej.2013.15
69. K. Baruch, A. Deczkowska, E. David, J. M. Castellano, O. Miller, A. Kertser, T. Berkutzki, Z. Barnett-Itzhaki, D. Bezalel, T. Wyss-Coray, I. Amit, M. Schwartz, Aging-induced type I interferon response at the choroid plexus negatively affects brain function. *Science* **346**, 89–93 (2014). Medline doi:10.1126/science.1252945
70. Y. Ziv, N. Ron, O. Butovsky, G. Landa, E. Sudai, N. Greenberg, H. Cohen, J. Kipnis,

M. Schwartz, Immune cells contribute to the maintenance of neurogenesis and spatial learning abilities in adulthood. *Nat. Neurosci.* **9**, 268–275 (2006). Medline doi:10.1038/nn1629
71. N. C. Derecki, A. N. Cardani, C. H. Yang, K. M. Quinnies, A. Crihfield, K. R. Lynch, J. Kipnis, Regulation of learning and memory by meningeal immunity: A key role for IL-4. *J. Exp. Med.* **207**, 1067–1080 (2010). Medline doi:10.1084/jem.20091419
72. H. Kim, B. Seed, The transcription factor MafB antagonizes antiviral responses by blocking recruitment of coactivators to the transcription factor IRF3. *Nat. Immunol.* **11**, 743–750 (2010). Medline doi:10.1038/ni.1897
73. C. J. Nirschl, C. G. Drake, Molecular pathways: Coexpression of immune checkpoint molecules: Signaling pathways and implications for cancer immunotherapy. *Clin. Cancer Res.* **19**, 4917–4924 (2013). Medline doi:10.1158/1078-0432.CCR-12-1972
74. S. Jung, J. Aliberti, P. Graemmel, M. J. Sunshine, G. W. Kreutzberg, A. Sher, D. R. Littman, Analysis of fractalkine receptor CX_3CR1 function by targeted deletion and green fluorescent protein reporter gene insertion. *Mol. Cell. Biol.* **20**, 4106–4114 (2000). Medline doi:10.1128/MCB.20.11.4106-4114.2000
75. C. A. Thaiss, D. Zeevi, M. Levy, G. Zilberman-Schapira, J. Suez, A. C. Tengeler, L. Abramson, M. N. Katz, T. Korem, N. Zmora, Y. Kuperman, I. Biton, S. Gilad, A. Harmelin, H. Shapiro, Z. Halpern, E. Segal, E. Elinav, Transkingdom control of microbiota diurnal oscillations promotes metabolic homeostasis. *Cell* **159**, 514–529 (2014). Medline doi:10.1016/j.cell.2014.09.048
76. U. Meyer, M. Nyffeler, S. Schwendener, I. Knuesel, B. K. Yee, J. Feldon, Relative prenatal and postnatal maternal contributions to schizophrenia-related neurochemical dysfunction after in utero immune challenge. *Neuropsychopharmacology* **33**, 441–456 (2008). Medline doi:10.1038/sj.npp.1301413
77. A. Agresti, A survey of exact inference for contingency tables. *Stat. Sci.* **7**, 131–153 (1992). doi:10.1214/ss/1177011454
78. C. Trapnell, L. Pachter, S. L. Salzberg, TopHat: Discovering splice junctions with RNA-seq. *Bioinformatics* **25**, 1105–1111 (2009). Medline doi:10.1093/bioinformatics/btp120
79. S. Heinz, C. Benner, N. Spann, E. Bertolino, Y. C. Lin, P. Laslo, J. X. Cheng, C. Murre, H. Singh, C. K. Glass, Simple combinations of lineage-determining transcription factors prime cis-regulatory elements required for macrophage and B cell identities. *Mol. Cell* **38**, 576–589 (2010). Medline doi:10.1016/j.molcel.2010.05.004
80. E. Eden, D. Lipson, S. Yogev, Z. Yakhini, Discovering motifs in ranked lists of DNA sequences. *PLOS Comput. Biol.* **3**, e39 (2007). Medline
81. E. Eden, R. Navon, I. Steinfeld, D. Lipson, Z. Yakhini, GOrilla: A tool for discovery and visualization of enriched GO terms in ranked gene lists. *BMC Bioinformatics* **10**, 48 (2009). Medline doi:10.1186/1471-2105-10-48
82. S. Picelli, A. K. Björklund, B. Reinius, S. Sagasser, G. Winberg, R. Sandberg, Tn5 transposase and tagmentation procedures for massively scaled sequencing projects. *Genome Res.* **24**, 2033–2040 (2014). Medline doi:10.1101/gr.177881.114
83. B. Langmead, C. Trapnell, M. Pop, S. L. Salzberg, Ultrafast and memory-efficient alignment of short DNA sequences to the human genome. *Genome Biol.* **10**, R25 (2009). Medline doi:10.1186/gb-2009-10-3-r25

ACKNOWLEDGMENTS

We thank members of the I.A. and M.S. labs for discussions. We thank Tali Wiesel for artwork. We thank Margalit Azoulay and Oz Rozenberg for animal handling. Research in the I.A. lab is supported by the European Research Council (309788), the Israeli Science Foundation (1782/11), the BLUEPRINT FP7 consortium, the Ernest and Bonnie Beutler Research Program of Excellence in Genomic Medicine, a Minerva Stiftung research grant, the Israeli Ministry of Science, Technology and Space, the David and Fela Shapell Family Foundation, and the National Human Genome Research Institute Center for Excellence in Genome Science (1P50HG006193). I.A. is the incumbent of the Alan and Laraine Fischer Career Development Chair. Research in the M.S. lab is supported by Advanced European Research Council grants (232835), by the EU Seventh Framework Program HEALTH-2011 (279017), M.S. holds the Maurice and Ilse Katz Professorial Chair in Neuroimmunology. M.H.S. was supported by grants from the 'Agence Nationale de la Recherche' (ANR BLAN07-1_205752, ANR-11-BSV3-026-01) and InCA (13-10/405/AB-LC-HS). He is a BIH-Einstein fellow, Fondation pour la Recherche Médicale (DEq. 20071210559 and DEq. 20110421320), and INSERM-Helmholtz group leader. D.W. is supported by the European Molecular Biology Organization (EMBO; ALT766-2014) and the European Commission FP7 (Marie Curie Actions, EMBOCOFUND2012, GA-2012-600394). ATAC-seq, ChIP-seq, bulk RNA-seq, and single cell RNA-seq data are deposited in GEO; accession number GSE79819.

SUPPLEMENTARY MATERIALS

www.sciencemag.org/cgi/content/full/science.aad8670/DC1
Materials and Methods
Figs. S1 to S8
Tables S1 to S10
References (*74*–*83*)

14 November 2015; accepted 10 June 2016
Published online 23 June 2016
10.1126/science.aad8670

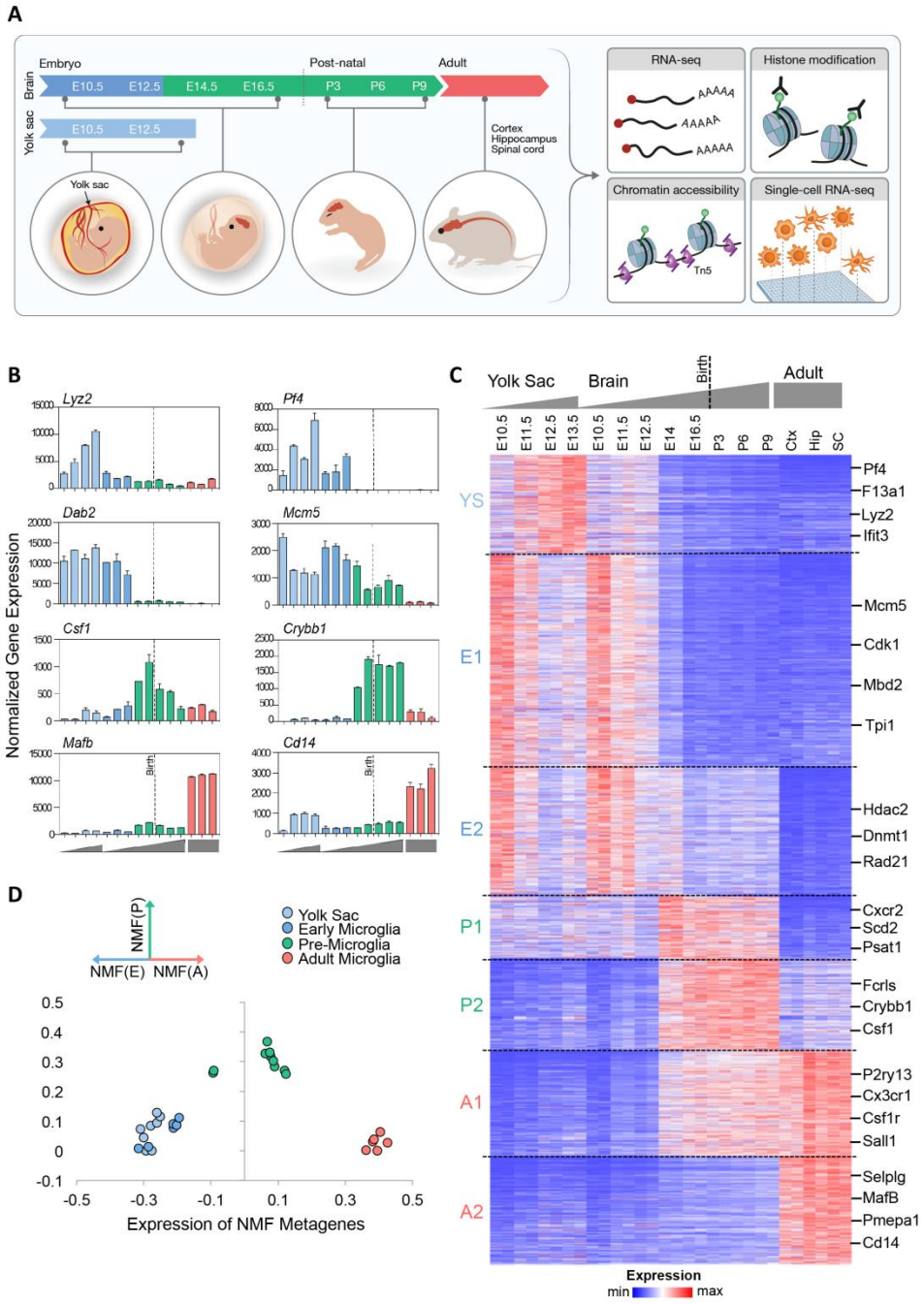

Fig. 1. Global gene expression patterns reveal distinct microglia developmental phases. (**A**) Schematic showing the multi-dimensional data collected throughout microglia development. (**B**) Bar graphs of expression for a representative set of gene markers across the course of microglia development as determined by RNA-seq. Error bars indicate standard error of the mean (SEM). (**C**) K-means clustering (k = 7; (*38*)) of 3059 genes with differential expression across the course of microglia development (Cortex=Ctx; Hippocampus=Hip; Spinal Cord=SC). (**D**) Nonnegative matrix factorization (NMF) analysis of gene expression revealed three meta-genes representing distinct transcriptional programs. Samples are color-coded by tissue and program (light blue=yolk sac; blue=early microglia; green=pre-microglia; red=adult microglia).

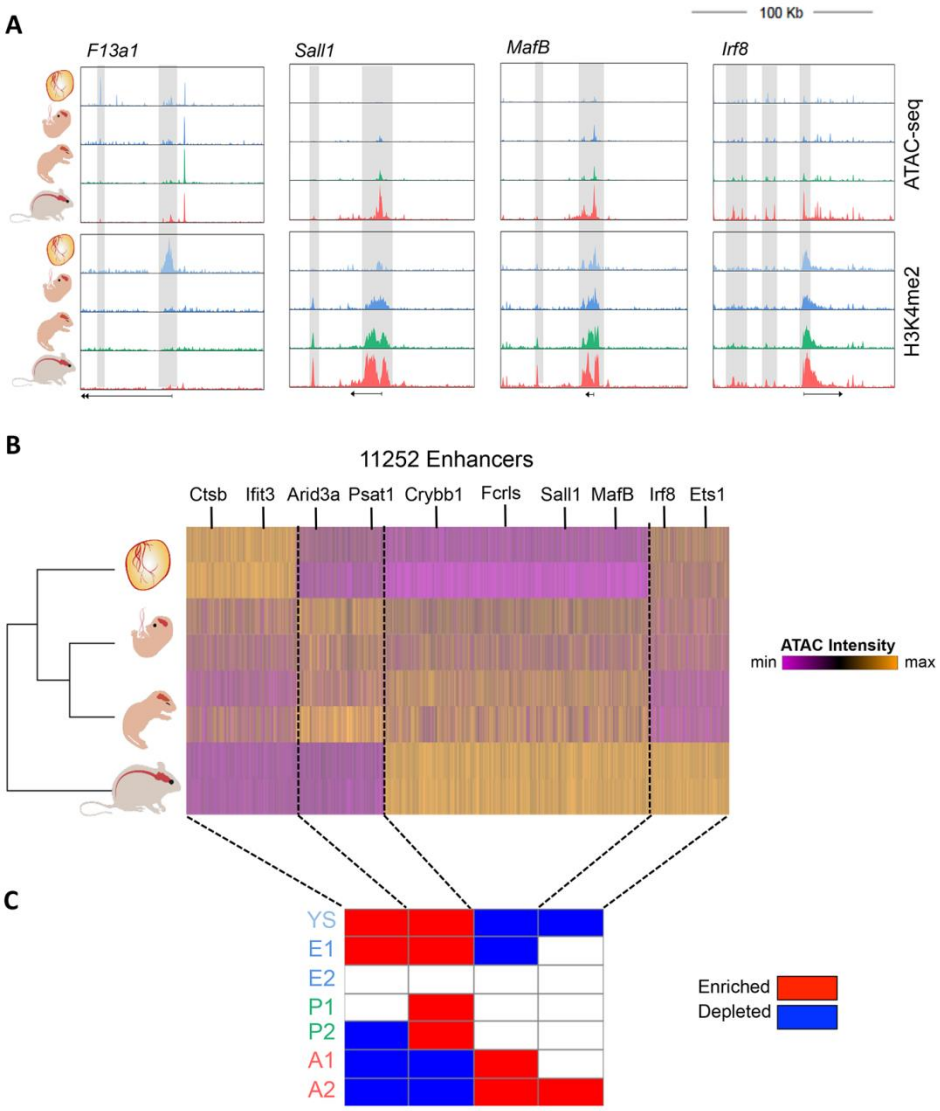

Fig. 2. Chromatin dynamics reflect distinct phases of microglia development. (**A**) Normalized profiles of H3K4me2 and ATAC-seq signal in 100 kilobase (kb) regions from YS progenitors (E12.5; light blue), early microglia (E12.5; blue), pre-microglia (P1; green) and adult (8wk; red) microglia. (**B**) K-means clustering (k = 4) of ATAC-seq intensity in distal K4me2 regions reveals 4 main categories of candidate enhancers. (**C**) Overlap between enhancer dynamics and gene expression clusters from Fig. 1C (enriched and depleted $P < 0.05$, Hypergeometric distribution).

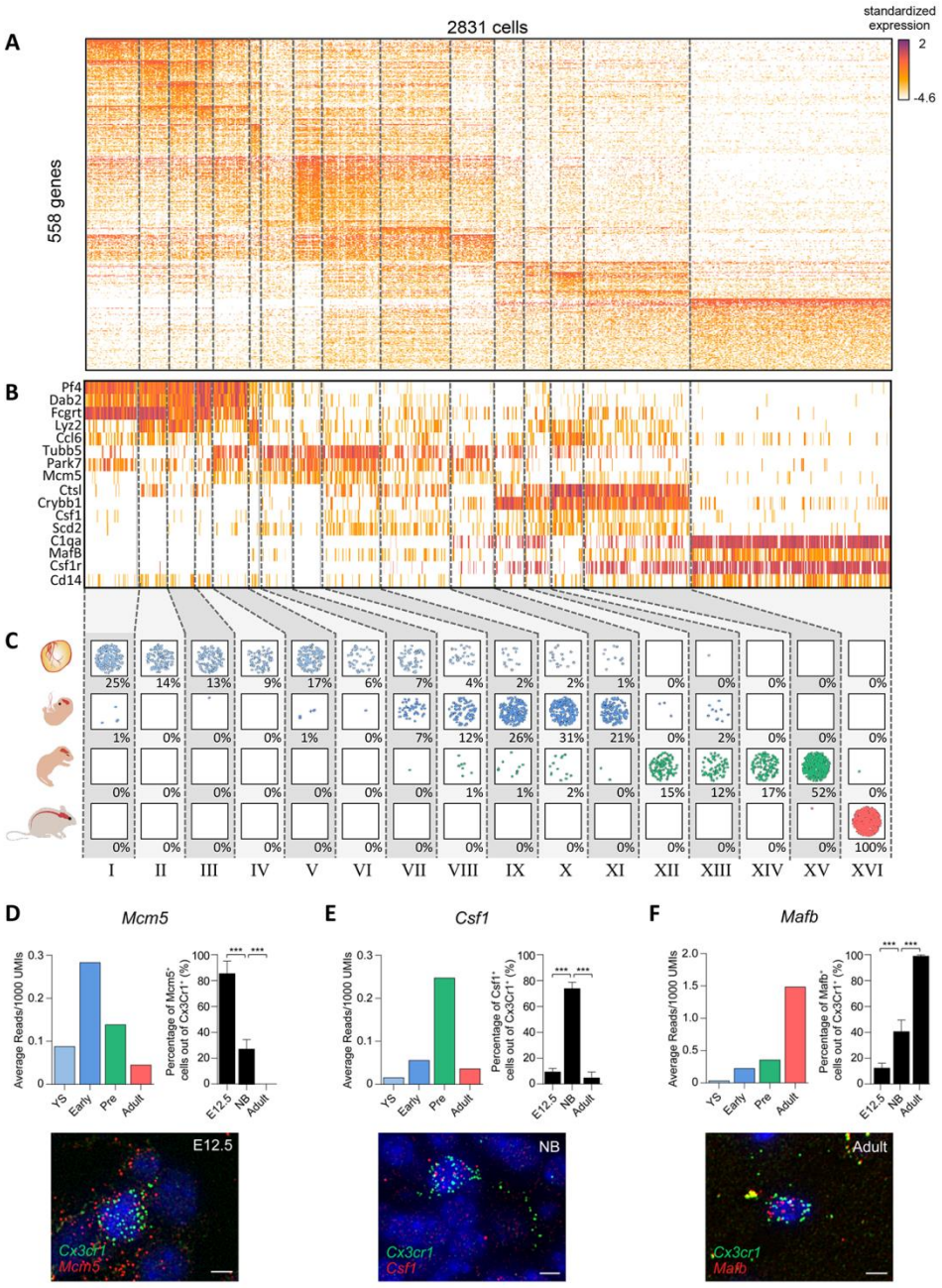

Fig. 3. Single cell RNA-seq shows homogeneity within phases of development. (**A**) Heatmap showing clustering (k = 16) of standardized expression of 558 most variable genes out of the 2071 total differential genes (methods) in 2831 individual cells isolated from yolk sac (E12.5), early microglia (E12.5), pre-microglia (E18.5) and adult microglia (8wk). (**B**) Representative set of marker genes differentially expressed between the different developmental stages. (**C**) Illustration of the number of cells from each sorted population that aligned to a given cluster defined in A. Percent of each population is given below each box. (**D**) Single molecule fluorescent in situ hybridization (smFISH) of mRNA molecules for *Mcm5*, a marker for early microglia, in intact brain tissue. Top left panel: Average expression of *Mcm5* across single cells from subpopulations associated with each developmental stage. Top right panel: Quantification of the percent of CX3CR1-GFP cells that overlap *Mcm5* RNA molecules (red). Bottom panel: Representative image of smFISH in an early brain section. (**E**) Same as (D), but for *Csf1*, a marker for pre-microglia. (**F**) Same as (D), but for *MafB*, a marker for adult microglia.

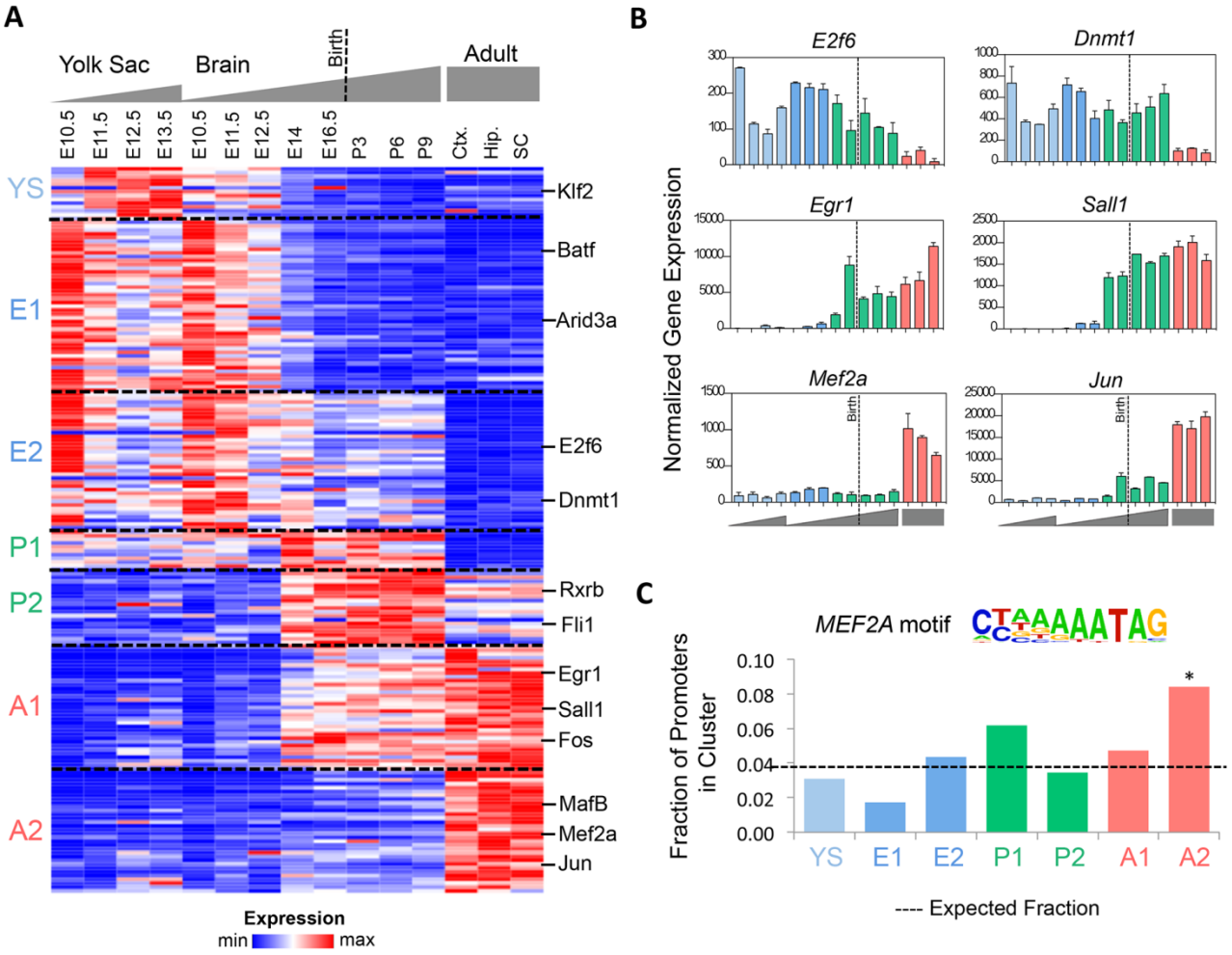

Fig. 4. Regulatory factors involved in each phase of microglia development. (**A**) Heatmap of gene expression of 190 transcription factors and chromatin modifiers from the clusters in Fig. 1C. (**B**) Bar graphs of expression for representative regulators across microglia development. Error bars indicate SEM. (**C**) Fraction of promoters associated with genes in each expression cluster (Fig. 1C) containing the sequence motif (logo shown) for MEF2A. Dashed line indicates the expected distribution of promoters. Significance of enrichment $P < 0.05$, Hypergeometric distribution.

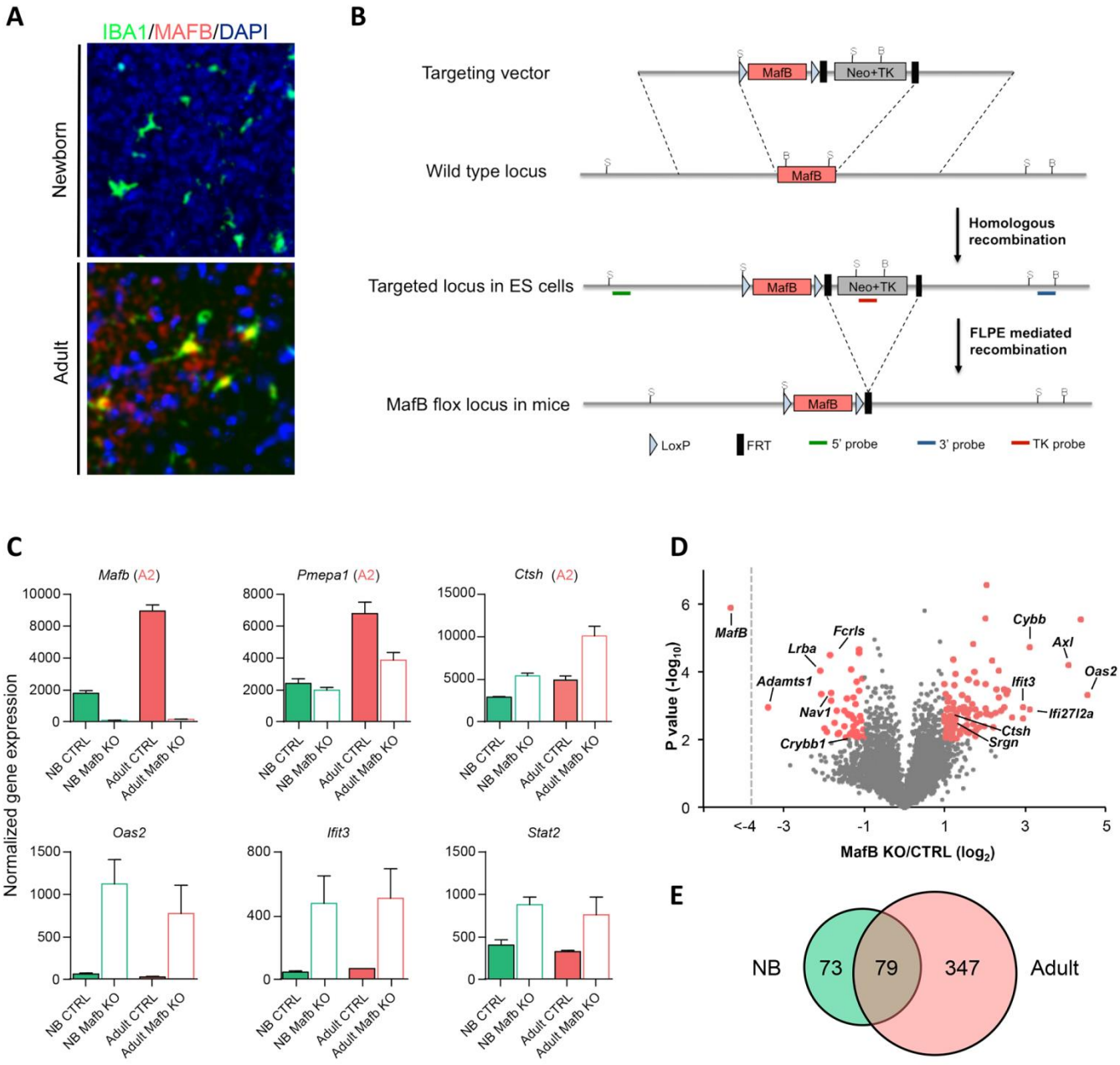

Fig. 5. MafB is critical for regulation of homeostasis in adult microglia. (**A**) Representative images of coronal sections from whole brains of mice showing overlap of immunostaining for Hoechst (blue), IBA-1 (green), and MAFB (red) [scale bar, 50 μm]. Sections taken from adult mice (8 weeks) demonstrate the co-expression of the microglia marker IBA-1, and the protein MAFB, while co-expression was not observed in pre-microglia (newborn). (**B**) MafB knockout mouse generation plot. (**C**) Expression of representative genes that are dysregulated in either pre- or adult microglia from MafB-knockout mice. Error bars indicate SEM. (**D**) Volcano plot showing the fold change and significance of genes between MafB-knockout and control microglia from adult mice. P-values determined by two-tailed *t* test. (**E**) Overlap in of differentially regulated genes from pre- (green) and adult (red) microglia.

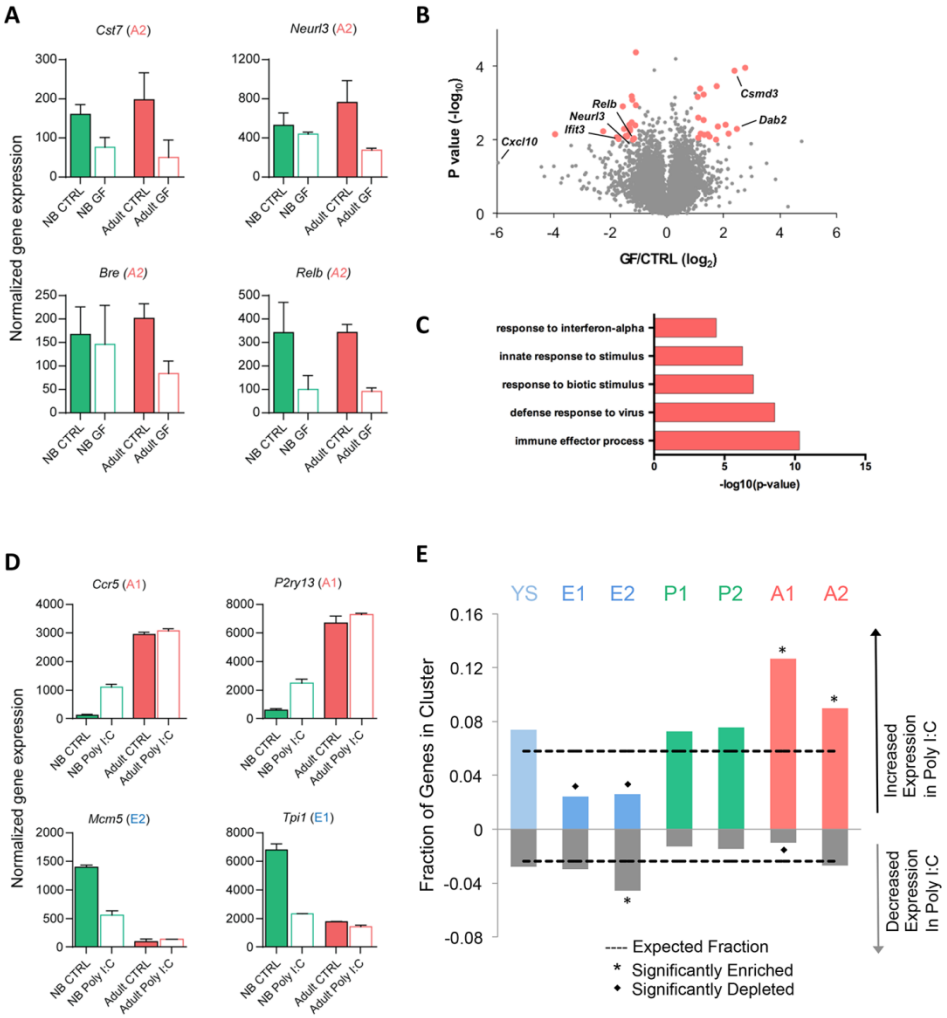

Fig. 6. Perturbations to immune signals shift microglia expression patterns. (**A**) Expression levels in microglia from newborn and adult germ-free mice compared to control. Shown are representative genes that are down-regulated in adult microglia. Error bars indicate SEM. (**B**) Volcano plot showing the fold change and significance of genes between germ-free and control microglia from adult mice. P-values determined by two-tailed *t* test. (**C**) Enrichment of gene ontology terms in adult down-regulated genes. (**D**) Expression levels in microglia from newborn and adult offspring of poly I:C injected (E14.5) mice compared to control (PBS-injected). Shown are representative genes that are differentially regulated in pre-microglia. The associated expression cluster from Fig. 1C is indicated. Error bars indicate SEM. (**E**) Fraction of genes in each expression cluster from Fig. 1C that were differentially regulated (at least 2-fold change) in pre-microglia from poly I:C relative to the control (PBS-injected). Dashed line indicates the expected distribution of genes. Significance of enrichment or depletion $P < 0.05$, Hypergeometric distribution.

Microglia development follows a stepwise program to regulate brain homeostasis

Orit Matcovitch-Natan, Deborah R. Winter, Amir Giladi, Stephanie Vargas Aguilar, Amit Spinrad, Sandrine Sarrazin, Hila Ben-Yehuda, Eyal David, Fabiola Zelada González, Pierre Perrin, Hadas Keren-Shaul, Meital Gury, David Lara-Astaiso, Christoph A. Thaiss, Merav Cohen, Keren Bahar Halpern, Kuti Baruch, Aleksandra Deczkowska, Erika Lorenzo-Vivas, Shalev Itzkovitz, Eran Elinav, Michael H. Sieweke, Michal Schwartz and Ido Amit (June 23, 2016)
published online June 23, 2016

Editor's Summary

Science (print ISSN 0036-8075; online ISSN 1095-9203) is published weekly, except the last week in December, by the American Association for the Advancement of Science, 1200 New York Avenue NW, Washington, DC 20005.